Dalton Transactions

Accepted Manuscript

ROYAL SOCIETY OF CHEMISTRY

www.rsc.org/dalton

Cite this: DOI: 10.1039/c0xx00000x

www.rsc.org/xxxxxx

ARTICLE TYPE

Alkali metal salts of formazanate ligands: diverse coordination modes as a result of the nitrogen-rich [NNCNN] ligand backbone

Raquel Travieso-Puente,[a] Mu-Chieh Chang[a] and Edwin Otten[a]*

Received (in XXX, XXX) XthXXXXXXXXX 20XX, Accepted Xth XXXXXXXXX 20XX

DOI: 10.1039/b000000x

Alkali metal salts of redox-active formazanate ligands were prepared, and their structures in the solid-state and solution determined. The nitrogen-rich [NNCNN] backbone of formazanates results in a varied coordination chemistry, with both the internal and terminal nitrogen atoms available for bonding with the alkali metal. The potassium salt K[PhNNC(*p*-tol)NNPh]·2THF (**1-K**) is dimeric in the solid state and even in THF solution, as a result of the K atom bridging *via* interaction with a terminal N atom and the aromatic ring of a second unit. Conversely, for the compounds Na[MesNNC(CN)NNMes]·2THF (**2-Na**) and Na[PhNNC(*t*Bu)NNPh] (**3-Na**) polymeric and hexameric structures are found in the solid state respectively. The preference for binding the alkali metal through internal N atoms (**1-K** and **2-Na**) to give a 4-membered chelate, or via internal/external N atoms (5-membered chelate in **3-Na**), contrasts the 6-membered chelate mode observed in our recently reported formazanate zinc complexes.

Introduction

Oxidative addition and reductive elimination are elementary reaction steps that are key to myriad (catalytic) transformations in organic and organometallic chemistry.[1] Such reactions typically occur at transition metal centres which possess two different oxidation states that can be reversibly addressed. Especially useful are transition metals for which there are two relatively stable oxidation states that differ by 2 electrons, so that odd-electron (radical) chemistry is avoided (e.g., the Pd(0)/Pd(II) redox couple in cross-coupling chemistry).[2] Despite the vast success of this type of chemistry, it mostly relies on relatively expensive and noble late transition elements such as those in the platinum group. Therefore, it is desirable to develop similar reactivity for cheap, earth-abundant first-row transition elements. A serious impediment in this regard is the tendency of the first-row transition elements to engage in (unselective) 1-electron redox-reactions. A potential strategy to mitigate this undesirable behaviour could be the use of an organic ligand scaffold that engages in redox-reactions. These so-called 'redox-active' ligands have gained prominence recently and several examples are known where such ligands play an important role in allowing unusual redox-reactivity to occur.[3-7]

Our efforts in this area have recently focussed on developing formazanates as redox-active ligands.[8, 9] The Gilroy group has recently reported formazanate boron complexes and studied their redox-properties by cyclic voltammetry.[10, 11] Monoanionic formazanate ligands (derived from the parent formazans) are close structural analogues of β-diketiminates. In contrast to β-diketiminates, which are a well-established and useful class of ligands in a wide range of coordination complexes and catalysts,[12] the transition metal chemistry of formazanate ligands remains largely unexplored. Considering possible synthesis routes to a variety of transition metal complexes containing formazanate ligands, we concluded that salt metathesis strategies would constitute a promising approach. Lithium, sodium and potassium salts are used most frequently in such reactions since the high lattice energy of the resulting alkali metal halides provides a large thermodynamic driving force. Here we describe the synthesis and structural features of several formazanate salts, which show a large structural diversity as a result of the nitrogen-rich [NNCNN] formazanate backbone. Formazanate ions are shown to bind to alkali metal cations to give 4- and 5-membered chelate rings. Further interactions with additional N-atoms from the NNCNN ligand backbone or a cyano substituent, or with an aromatic moiety leads to unusual dimeric, hexameric or polymeric aggregates.[13-16]

Results and Discussion

Solid-state Structures. Three different formazans (**1-H** – **3-H**) were synthesized using published procedures.[17-19] Subsequent treatment with sodium or potassium hydride under anhydrous conditions allowed for the synthesis and structural characterization of the corresponding formazanate salts, which were obtained in reasonable to good yields as intensely coloured solid products (Scheme 1). Deprotonation of the neutral formazan PhNNC(*p*-tol)NNHPh (**1-H**) is readily achieved by stirring a THF solution of **1-H** with potassium hydride as evidenced by a rapid colour change from dark red to violet and evolution of H_2 gas. Crystallization of the resulting potassium salt was achieved by slow diffusion of hexane into a THF solution of the product to yield K[PhNNC(*p*-tol)NNPh]·2THF (**1-K**). While single crystal

X-ray analysis confirmed the formation of the desired potassium formazanate salt, the structure shows some surprising features (Figure 1, pertinent bond distances and angles in Table 1). In contrast to alkali metal salts of the structurally related β-diketiminates (which bind the alkali metal through the *N*CCC*N* atoms to give 6-membered chelate rings), the formazanate anion in compound **1-K** is bound through the internal nitrogen atoms (N*N*C*N*N) of the ligand backbone to give rise to a 4-membered chelate ring with K(1)-N(2) and K(1)-N(3) bond distances of 2.8723(16) and 2.9270(17) Å, respectively. One of the terminal N atoms (N4) interacts with a potassium atom of another (formazanate)K fragment to result in a dimeric structure. In addition, two carbon atoms of the *p*-tolyl ring show a close approach to this K atom with K-C(8) and K-C(9) distances of 3.2448(19) and 3.292(2) Å, respectively.

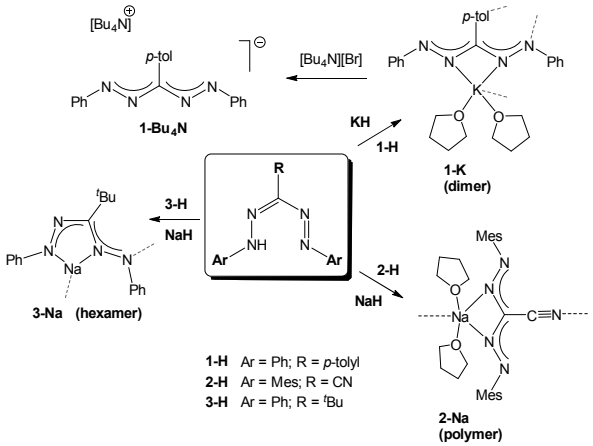

Scheme 1. Synthesis of alkali metal formazanate salts.

The interaction between (metal) cations and electron-rich π-systems (cation-π interactions) constitutes an important class of non-covalent interaction that has widespread application, including in biological systems.[20] Also in the coordination chemistry of main group metals to organic ligands, this type of interactions can greatly affect the structures, stability and reactivity of the resulting complexes.[21-25] In the case of **1-K**, the interaction between the potassium cation and the *p*-tolyl moiety leads to a dramatic stabilization of the dimeric structure, such that it remains intact even in THF solution (vide infra).

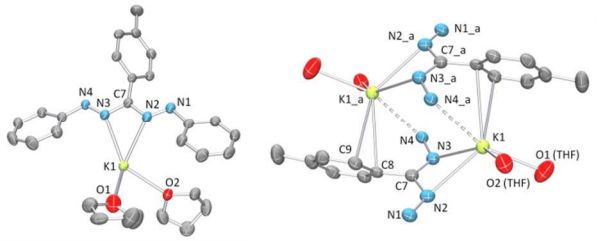

Figure 1. X-ray structure of **1-K**: asymmetric unit (left) and core of the dimeric structure (right) showing 50% probability ellipsoids. Hydrogen atoms are omitted for clarity.

Deprotonation of the cyano-substituted formazan MesNNC(CN)NNHMes (**2-H**) with NaH or KH allows isolation of a the formazanate products M[MesNNC(CN)NNMes]]·xTHF (M = Na; x = 2 (**2-Na**), M = K; x = 0 (**2-K**)) in good yield as orange powders that are insoluble in aromatic and aliphatic solvents. The number of THF molecules bound to the alkali metal center was determined by analysis of the ^{1}H NMR spectra: in case of **2-K**, no THF was present, while for **2-Na** the NMR suggests two molecules of THF are coordinated. We were unable to obtain crystals of **2-K**, so its solid state structure is unknown. However, based on the observation of K^+-arene interactions in the structure of **1-K**, it is tempting to conclude that the coordination sphere around the potassium atom in **2-K** is complemented by interactions with the Mes ring(s). The X-ray crystal structure of a related base-free β-diketiminate potassium salt has been reported in the literature.[21] In the case of **2-Na**, crystalline material was obtained by recrystallization from THF/hexane. X-ray analysis shows that **2-Na** is a coordination polymer in which the cyano group is bridging to a second (formazanate)Na unit, resulting in a linear polymer chain in which the C(102)-C(112)-N(32)-Na(1) atoms reside on a crystallographic C_2 axis (Figure 2, pertinent bond distances and angles in Table 1). Each sodium atom is coordinated by the internal nitrogens of the formazanate fragment to give a 4-membered chelate ring, as is observed in **1-K**. In contrast to **1-K**, the terminal N-atoms in **2-Na** do not engage in further M-N interactions. The Na-N(formazanate) distances are 2.4563(11) and 2.4840(10) Å for Na(1)-N(21) and Na(2)-N(22), respectively, and the bonding within each formazanate ligand is fully symmetric as imposed by the crystallographic twofold symmetry. Two THF molecules and the cyano group complete the coordination sphere around each Na atom to give 5-coordinate geometry. The Na-N(cyano) distances are 2.3612(15) and 2.3732(15) Å, while Na-O(THF) distances vary between 2.3412(8) and 2.3878(9) Å. Unlike the situation in **1-K**, there are no additional interactions between the aromatic moieties and the metal found in the solid state structure of **2-Na**, which reflects the smaller size of Na compared to K, its lower π-philicity[26] and the increased steric demands of the mesityl rings. The equivalent N-N and N-C bond lengths within the ligand backbone indicate full delocalization of the negative charge of the formazanate anion.

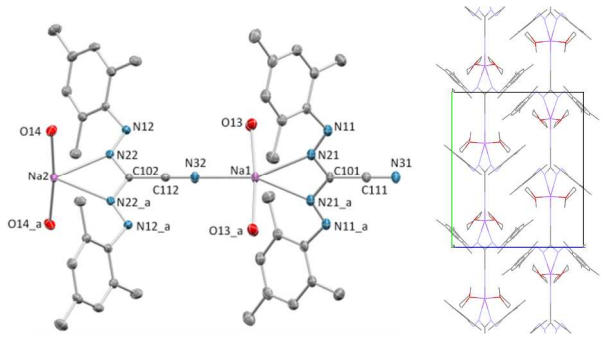

Figure 2. X-ray structure of **2-Na**: molecular structure (left) showing 50% probability ellipsoids, and packing diagram (view along a-axis, right). Hydrogen atoms and THF molecules (except O atoms) are omitted for clarity.

Deprotonation of **3-H** with NaH in THF afforded the product **3-Na$_{THF}$** upon removal of the solvent. According to NMR, two molecules of THF are coordinated to this material. In contrast to compounds **1-K** and **2-Na**/**K**, which are very insoluble in aliphatic/aromatic solvents, the product **3-Na$_{THF}$** is quite soluble in toluene and crystals suitable for X-ray analysis were obtained from toluene/hexane. The compound Na[PhNNC(^{t}Bu)NNPh] (**3-Na**) crystallizes from this solvent mixture without any THF

Table 1. Selected bond distances and angles in compounds **1-K**, **2-Na**, **3-Na**, and **1-Bu$_4$N**

	1-K	**2-Na**[a]		**3-Na**	**1-Bu$_4$N**
M(1) – N(1)				2.4006(11)	
M(1) – N(2)	2.9270(17)	2.4563(11)	2.4840(10)		
M(1) – N(3)	2.8723(16)			2.4192(11)	
M(1) – N(4_a)	2.9342(17)			2.5754(11)	
N(1) – N(2)	1.285(2)	1.2809(14)	1.2810(13)	1.3033(14)	1.2987(19)
N(3) – N(4)	1.306(2)			1.3170(14)	1.3036(18)
N(2) – C[b]	1.357(3)	1.3632(12)	1.3633(12)	1.3549(15)	1.363(2)
N(3) – C[b]	1.347(3)			1.3465(15)	1.357(2)

[a] The labelling scheme for **2-Na** includes a suffix (1 or 2) for the C and N atoms due to the presence of two independent formazanate(Na) (e.g., Na(1)-N(21) and Na(2)-N(22)). [b] The central carbon in the ligand backbone: C(101) and C(102) in case of **2-Na**, C(7) for all others.

coordinated to the Na centre. The resulting structure is a hexameric aggregate of (formazanate)Na units (Figure 3, pertinent bond distances and angles in Table 1). The Na cation is surrounded by the N(1) (terminal) and N(3) (internal) nitrogen atoms of a formazanate fragment to result in a 5-membered chelate ring. Its coordination sphere is complemented by N(4) of a second formazanate ligand. Additional weak interactions between Na and the *ortho*-C of the phenyl ring are observed with a Na(1)-C(6) distance of 3.0080(13) Å. Interactions between hexameric units are observed in the {Na(formazanate)}$_6$ plane, resulting in a 2D network (see Figure 3) that is held together by cation-π interactions.

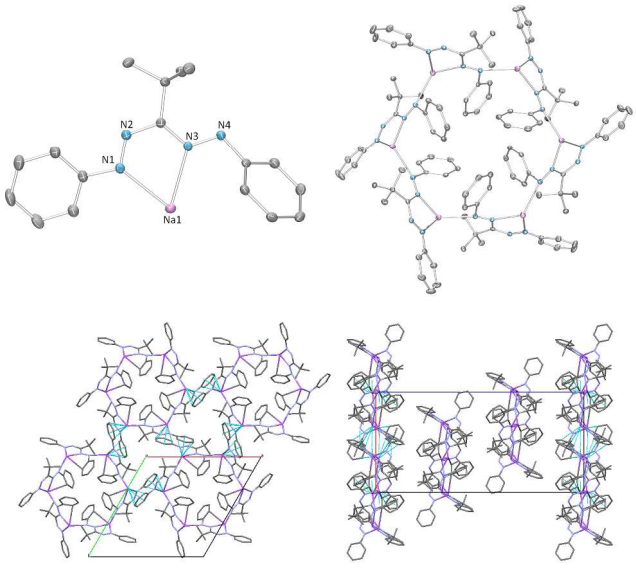

Figure 3. X-ray structure of **3-Na**: molecular structure (asymmetric unit, top left), hexameric aggregate (top right) showing 50% probability ellipsoids. Packing diagram showing the cation-π interactions as cyan dotted lines (view along c, bottom left; along b, bottom right). Hydrogen atoms are omitted for clarity.

With the structural data shown above, it was established that both 4- and 5-membered chelate rings are possible upon coordination of the formazanate NNCNN-framework to alkali metal cations. The recent work by Hicks and co-workers[18, 27, 28] and our group[8, 9] and some older examples of metal formazanate complexes[29-34] show that in most of the cases a 6-membered chelation mode analogous to that observed for *β*-diketiminate complexes is preferred, but this apparently is not favourable for very ionic compounds as described here. We became interested in the structure of formazanate anions devoid of a coordinating metal cation. A salt metathesis reaction between **1-K** and [Bu$_4$N][Br] cleanly affords the ionic compound [Bu$_4$N][PhNNC(*p*-tol)NNPh] (**1-Bu$_4$N**), which may be obtained in crystalline form by diffusion of hexane into a THF solution. The solid state structure of **1-Bu$_4$N** (Figure 4, pertinent bond distances and angles in Table 1) shows no interaction between the tetrabutyl ammonium cation and formazanate anion. The bond distances within the formazanate backbone are indicative of a fully delocalized structure with N-N and N-C bond lengths that are statistically indistinguishable. The observation that a 'linear' conformation is formed in the absence of a bound metal center suggests that electrostatic repulsions are minimized in this situation.

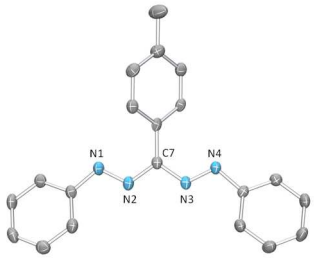

Figure 4. X-ray structure of **1-Bu$_4$N** showing 50% probability ellipsoids, hydrogen atoms and the [Bu$_4$N]$^+$ fragment omitted for clarity.

NMR studies: solution structures. Having established the solid state structure of a series of formazanate salts, we now turn to the characterization of these compounds in solution. The potassium salt **1-K** is insoluble in C_6D_6 but dissolves reasonably well in THF-d_8. ^{1}H NMR analysis of a THF-d_8 solution of **1-K** shows broadened resonances at room temperature. A series of (2D) NMR spectra was recorded between -60 and 80 °C in order to elucidate the structure of **1-K** in solution (see Figure 5 for representative ^{1}H NMR spectra). At 80 °C, the ^{1}H NMR spectrum is consistent with a C_{2v} symmetric structure with equivalent N-Ph moieties and 2 sets of resonances for the *p*-tolyl CH groups. Even at this temperature, one of these (presumably the *p*-tolyl *o*-CH) is broadened due to dynamic exchange. Upon cooling the NMR tube in the spectrometer to 0 °C or below, the number of resonances in the aromatic region is doubled (to a total of 10), which results from splitting of each resonance into 2 components with a 1:3 ratio. A series of 2D NMR experiments at -25 °C (see Experimental Section for details) allowed assignment of all peaks and indicates that **1-K** retains a dimeric structure in THF solution. Based on the observation of a 1:3 ratio for all aromatic signals (Ph and *p*-tolyl groups) even down to -60 °C it is concluded that in solution only one potassium atom is bridging the two formazanate ligands to give an asymmetric dimeric compound (Figure 6). In this structure the hydrogen atom sites that correspond to the smaller fraction are those that are in proximity of the coordinated potassium atom (shown in red in Figure 6), i.e. 2 of the *p*-tolyl CH groups (out of 8 total) and the N-Ph group (1 of the 4) where K is bound. The 'free' N-Ph and *p*-tolyl groups are apparently not sufficiently different to be observed separately.

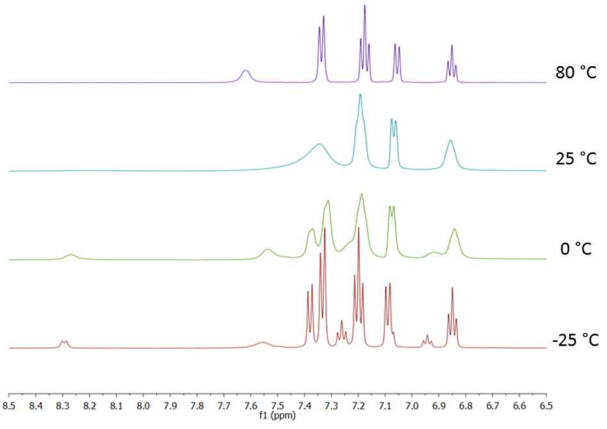

Figure 5. Variable-temperature ^{1}H NMR spectra of **1-K**.

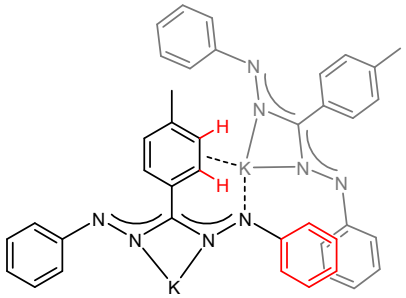

Figure 6. Schematic representation of the solution structure of **1-K** (THF molecules omitted for clarity), highlighting the 1:3 ratio of resonances observed (red:black).

A dynamic equilibrium between the sites of K-coordination is evidenced by exchange cross-peaks in the EXSY spectrum at -25 °C; all resonances that are affected by coordination of the potassium ion (see Figure 6) show exchange with those that are 'free'. Upon increasing the temperature, broadening and eventually coalescence of the two sets of resonances is observed to obtain (averaged) C_{2v} symmetry.

NMR characterization of **1-Bu$_4$N** in THF-d_8 shows that the appearance of the ^{1}H spectrum is quite different compared to **1-K**: the resonances are much sharper at room temperature, and chemicals shifts in the aromatic region are different. Most notably, the ^{13}C NMR shift of the central NCN carbon atom appears at 153.17 ppm for **1-Bu$_4$N**, which is shifted downfield by ~ 4.3 ppm relative to that in **1-K** in line with what would be expected by removal of the coordinating cation.

The alkali-metal salts of formazanates **2** and **3** are much more soluble in THF-d_8, which indicates that the aggregates observed in the solid state are easily broken by the donor solvent. For **2-Na** and **2-K**, the NMR spectra are virtually identical suggesting that in THF solution the compounds exist primarily as solvent-separated ion-pairs: there is no influence of the alkali metal cation on the chemical shifts of the formazanate anion. For compound **3-Na**, crystals of the hexameric aggregate that do not contain THF are sparingly soluble in C_6D_6. Its ^{1}H NMR spectrum is consistent with a symmetric structure in which both Ph groups are equivalent. It is not clear from these data what the aggregation state of **3-Na** is in this case, but it seems likely based on its solubility that the hexameric aggregate observed in the solid state is broken up in solution.

Conclusions

We have shown that formazanate alkali metal salts are accessible in a straightforward manner by deprotonation of the parent formazans with NaH or KH. The solid state structure of several derivatives was determined and shown to favour coordination of the alkali metal cation to the internal nitrogen atoms of the formazanate [NNCNN] ligand backbone in most cases. The sodium salt of [PhNNC(^{t}Bu)NNPh]$^-$ forms an unusual hexameric structure in which the Na atom is bound in an asymmetric fashion through an internal and terminal N atom. These finding contrast the 6-membered chelate rings that have been previously observed from coordination of the terminal nitrogen atoms to (transition) metal centres. We anticipate that the versatile coordination behaviour due to the nitrogen-rich backbone of formazanates will lead to transition metal complexes with flexible coordination environment that can adapt their steric profile to (for example) accommodate binding of substrates. In combination with the established redox-active nature of formazanates, these features could be useful in transition metal catalysis. The synthesis of alkali metal formazanate salts described herein presents an opportunity for their use in salt metathesis with transition metal salts, the products of which could find subsequent application in (redox-)catalysis. Work in this direction is currently underway in our laboratory.

Experimental Section

General Considerations. All manipulations were carried out

under nitrogen atmosphere using standard glovebox, Schlenk, and vacuum-line techniques. Toluene, pentane and hexane (Aldrich, anhydrous, 99.8%) were passed over columns of Al_2O_3 (Fluka), BASF R3-11-supported Cu oxygen scavenger, and molecular sieves (Aldrich, 4 Å). THF (Aldrich, anhydrous, 99.8%) was dried by percolation over columns of Al_2O_3 (Fluka). All solvents were degassed prior to use and stored under nitrogen. C_6D_6 and THF-d_8 (Aldrich) were vacuum transferred from Na/K alloy and stored under nitrogen. $[Bu_4N]Br$ (Sigma-Aldrich) was used as received, NaH (Sigma-Aldrich, 60 % dispersion in mineral oil) and KH (Sigma-Aldrich, 30 wt% dispersion in mineral oil) were washed several times with hexane to free from mineral oil and subsequently dried *in vacuo* to obtain a fine powder. The compounds PhNNC(*p*-tolyl)NNHPh (**1-H**),[18] MesNNC(CN)NNHMes (**2-H**)[19] and PhNNCH(^{t}Bu)NNPh (**3-H**)[17] were prepared via literature procedures.

Synthesis of K[PhNNC(*p*-tol)NNPh]·2THF (1-K). To a mixture of **1-H** (2.00 g, 6.36 mmol) and KH (306 mg, 7.63 mmol) was added 40 mL of THF. Gas evolution was observed immediately and the color changed from dark red to violet. After stirring at room temperature for 16 h, the solution was separated from solid material by centrifugation and the clear supernatant was transferred to a clean flask. Removal of all volatiles and subsequent washing with hexane afforded 2.76 g of **1-K** as a dark purple powder (5.56 mmol, 87%). Crystals suitable for X-ray analysis were obtained by slow diffusion of hexane into a THF solution of **1-K**. ^{1}H NMR (THF-d_8, 80 ºC, 500 MHz): δ 7.65 (br, 2H, *p*-tol *o*-H), 7.33 (d, 4H, *J* = 7.8, Ph *o*-H), 7.15 (t, 4H, *J* = 7.6, Ph *m*-H), 7.02 (d, 2H, *J* = 7.8, *p*-tol *m*-H), 6.82 (t, 2H, *J* = 7.2, Ph *p*-H), 3.62 (m, 4H, THF), 2.29 (s, 3H, CH_3), 1.77 (m, 4H, THF). ^{13}C NMR (THF-d_8, 80 ºC, 126 MHz): δ 158.54 (s, Ph *ipso*-C), 134.68 (s, *p*-tol *p*-C), 130.78 (br d, *p*-tol *o*-CH), 129.14 (d, Ph *m*-CH), 127.95 (d, *p*-tol *m*-CH), 122.64 (d, Ph *p*-CH), 120.39 (Ph *o*-CH), 67.45 (THF), 25.37 (THF), 21.45 (q, CH_3). The N*C*N and *p*-tol *ipso*-C were not observed.
^{1}H NMR (THF-d_8, -20 ºC, 500 MHz): δ 8.25 (br d, 1H, *J* = 7.6, *p*-tol *o*-H), 7.52 (br, 2H, Ph *o*-H), 7.33 (d, 3H, *J* = 7.5, *p*-tol *o*-H), 7.29 (d, 6H, *J* = 7.7, Ph *o*-H), 7.22 (t, 2H, *J* = 7.4, Ph *m*-H), 7.16 (t, 6H, *J* = 7.4, Ph *m*-H), 7.05 (d, 4H, *J* = 7.4, *p*-tol *m*-H), 6.90 (t, 1H, *J* = 7.2, Ph *p*-CH), 6.82 (t, 3H, *J* = 7.1, Ph *p*-CH). ^{13}C NMR (THF-d_8, -20 ºC, 126 MHz): δ 158.05 (Ph *ipso*-C), 157.42 (NCN), 135.25 (*p*-tol *p*-C), 133.92 (*p*-tol *ipso*-C), 132.21 (*p*-tol *o*-CH), 129.42 (Ph *m*-CH), 129.26 (Ph *m*-CH), 128.25 (*p*-tol *m*-H), 128.03 (*p*-tol *m*-H), 123.40 (Ph *p*-CH), 122.50 (Ph *p*-CH), 120.78 (Ph *o*-H), 120.21 (Ph *o*-H), 68.39 (THF), 26.54 (THF), 21.84 (CH_3). Anal. calcd. for $C_{28}H_{33}N_4KO_2$: C 67.71, H 6.70, N 11.28; found: C 67.74, H 6.62, N 11.31.

Synthesis of K[MesNNC(CN)NNMes] (2-K). To a mixture of **2-H** (1.86 g, 5.58 mmol) and KH (265 mg, 6.63 mmol) was added 30 mL of THF. After stirring at room temperature overnight, the supernatant was separated by centrifugation and evaporated to dryness. The residue was washed with toluene (10 mL) and hexane (10 mL) and subsequently dried *in vacuo* to give **2-K** as a dark orange powder (1.95 g, 5.25 mmol, 94%). Attempts to obtain crystalline material were unsuccessful. ^{1}H NMR (THF-d_8, 25 ºC, 500 MHz): δ 6.72 (s, 2H, Mes *m*-H), 2.24 (s, 6H, Mes *o*-CH_3), 2.20 (s, 3H, Mes *p*-CH_3). ^{13}C NMR (THF-d_8, 25 ºC, 126 MHz): δ 152.27 (Mes *ipso*-C), 132.71 (Mes *p*-C), 130.32 (Mes *o*-C), 129.88 (Mes *m*-CH), 129.47 (NCN), 116.56 (CN), 21.17 (Mes *p*-CH_3), 19.71 (Mes *o*-CH_3). A satisfactory elemental analysis could not be obtained.

Synthesis of Na[MesNNC(CN)NNMes]·2THF (2-Na). A mixture of **2-H** (85 mg, 0.26 mmol) and NaH (10 mg, 0.41 mmol) was dissolved in THF (20 mL), and H_2 gas evolution was observed immediately. The reaction mixture was stirred overnight. After the solvent was removed, a new portion of THF was added and the solution was filtered to separate from excess NaH. The solvents was removed from the extract to give **2-Na** as a pure orange powder (107 mg, 0.22 mmol, 85 %). Recrystallization from THF/hexane gave crystals suitable for X-ray analysis. ^{1}H NMR (THF-d_8, 25 ºC, 500 MHz): δ 6.71 (s, 4H, Mes *m*-CH), 3.62 (m, 4H, THF), 2.25 (s, 12H, Mes *o*-CH_3), 2.20 (s, 6H, Mes *p*-CH_3), 1.78 (m, 4H, THF). ^{13}C NMR (THF-d_8, 25 ºC, 126 MHz): δ 152.12 (Mes *ipso*-C), 132.68 (Mes *p*-C), 130.43 (Mes *o*-C), 129.86 (Mes *m*-CH), 128.94 (NCN), 116.99 (C≡N), 68.39 (THF), 25.56 (THF), 21.16 (Mes *p*-CH_3), 19.88 (Mes *o*-CH_3). Anal. calcd. for $C_{28}H_{38}N_5NaO_2$: C, 67.31; H, 7.67; N, 14.02; found: C 67.02, H 7.61, N 14.05.

Synthesis of Na[PhNNC(^{t}Bu)NNPh]·THF (3-Na_{THF}). A mixture of **3-H** (1.00 g, 3.64 mmol) and NaH (140 mg, 5.83 mmol) was dissolved in THF (20 mL), and H_2 gas evolution was observed straightaway with a rapid colour change from orange to dark violet. The mixture was stirred overnight. The solvent was subsequently evaporated. The residue was extracted into THF and the solution filtered to separate from excess NaH. Upon removal of the solvent, **3-Na_{THF}** was obtained as an intensely colored (dark blue/black) powder (709 mg, 1.89 mmol, 52 %). Attempts to obtain crystalline material were unsuccessful. ^{1}H NMR (C_6D_6, 25 ºC, 500 MHz): δ 7.47 (d, 4H, *J* = 7.6, Ph *o*-H), 7.24 (t, 4H, *J* = 7.5, Ph *m*-H), 6.94 (t, 2H, *J* = 7.0, Ph *p*-H), 3.21 (THF), 1.91 (s, 9H, ^{t}Bu), 1.20 (THF). ^{13}C NMR (C_6D_6, 25 ºC, 126 MHz): δ = 158.51 (Ph *ipso*-C), 156.38 (NCN),129.88 (Ph *m*-CH), 123.75 (Ph *p*-CH), 119.97 (Ph *o*-CH), 68.27 (THF), 39.02 ($\underline{C}(CH_3)_3$), 30.53 ($C(\underline{C}H_3)_3$), 25.75 (THF). A satisfactory elemental analysis could not be obtained.

Synthesis of Na[PhNNC(^{t}Bu)NNPh] (3-Na). A sample of **3-Na_{THF}** was recrystallized from toluene/pentane to give dark blue hexagonal crystals suitable for X-ray analysis. ^{1}H NMR (C_6D_6, 25 ºC, 400 MHz): δ 7.26 (t, 4H, *J* = 7.4, Ph *o*-H), 7.22 (d, 4H, *J* = 7.6, Ph *m*-H), 6.98 (t, 2H, *J* = 7.1, Ph *p*-H), 1.85 (s, 9H, ^{t}Bu). Despite repeated attempts, a satisfactory elemental analysis could not be obtained.

Synthesis of [Bu_4N][PhNNC(*p*-tol)NNPh] (1-Bu_4N). A mixture of **1-K** (292 mg, 0.59 mmol) and $[Bu_4N]Br$ (191 mg, 0.59 mmol) was dissolved in THF (20ml). The mixture was stirred overnight. After that the solvent was removed, and a new portion of THF was added to extract the product, giving a fuchsia solution. After removal of the solvent, crystals suitable for x-ray analysis could be obtained from slow diffusion of hexane into the THF solution (313 mg, 0.56 mmol, 95% yield). ^{1}H NMR (THF-d_8, 60 ºC, 500

MHz): δ 7.74 (d, 2H, J = 7.4, *p*-tol *o*-H), 7.44 (d, 4H, J = 7.6, Ph *o*-H), 7.10 (t, 4H, J = 7.2, Ph *m*-H), 6.98 (d, 2H, J = 7.4, *p*-tol *m*-H), 6.74 (t, 2H, J = 7.0, Ph *p*-H), 2.77 (m, 8H, Bu α-CH_2), 2.28 (s, 3H, *p*-tolyl CH_3), 1.22 (m, 8H, Bu β-CH_2), 1.13 (m, 8H, Bu γ-CH_2), 0.78 (m, 12H, Bu δ-CH_3).^{13}C NMR (THF-d_8, 60 ºC, 126 MHz): δ 158.63 (Ph *ipso*-C), 153.17 (N*C*N), 134.06 (*p*-tol *p*-C), 133.91 (*p*-tol *ipso*-C), 131.83 (*p*-tol *o*-CH), 128.92 (Ph *m*-CH), 127.59 (*p*-tol *m*-CH), 122.11 (Ph *p*-CH), 120.89 (Ph *o*-CH), 59.21 (Bu α-CH_2), 24.75 (Bu β-CH_2), 21.61 (*p*-tolyl CH_3), 20.51 (Bu γ-CH_2), 14.03 (Bu δ-CH_3). Anal.calcd. for $C_{36}H_{53}N_5$: C, 77.79; H, 9.61; N, 12.60; found: C,77.91; H, 9.75; N, 12.56.

X-ray crystallography. Suitable crystals of **1-K**, **2-Na**, **3-Na** and **1-Bu$_4$N** were mounted on a cryo-loop in a drybox and transferred, using inert-atmosphere handling techniques, into the cold nitrogen stream of a Bruker D8 Venture diffractometer. The final unit cell was obtained from the xyz centroids of 9865 (**1-K**), 9965 (**2-Na**), 9894 (**3-Na**), and 6731 (**1-Bu$_4$N**) reflections after integration. Intensity data were corrected for Lorentz and polarisation effects, scale variation, for decay and absorption: a multiscan absorption correction was applied, based on the intensities of symmetry-related reflections measured at different angular settings (*SADABS)*.[35] The structures were solved by direct methods using the program *SHELXS*.[36] The hydrogen atoms were generated by geometrical considerations and constrained to idealised geometries and allowed to ride on their carrier atoms with an isotropic displacement parameter related to the equivalent displacement parameter of their carrier atoms. Structure refinement was performed with the program package *SHELXL*.[36] Crystal data and details on data collection and refinement are presented in Table 2.

Table 2. Crystallographic data for **1-K**, **2-Na**, **3-Na** and **1-Bu$_4$N**

	1-K	**2-Na**	**3-Na**	**1-Bu$_4$N**
chem formula	$C_{56}H_{66}K_2N_8O_4$	$C_{28}H_{38}N_5NaO_2$	$C_{17}H_{19}N_4Na$	$C_{36}H_{53}N_5$
M_r	993.36	499.62	302.36	555.86
cryst syst	monoclinic	monoclinic	trigonal	monoclinic
color, habit	dark violet, platelet	orange, block	dark purple, block	violet, needle
size (mm)	0.45 x 0.22 x 0.08	0.28 x 0.24 x 0.11	0.26 x 0.21 x 0.06	0.30 x 0.13 x 0.05
space group	*P2$_1$/n*	*P2/c*	*R-3*	*P2$_1$/n*
a (Å)	9.4184(5)	13.1681(6)	16.7609(8)	8.5964(5)
b (Å)	16.0507(10)	15.7367(7)	16.7609(8)	19.7591(14)
c (Å)	17.5178(10)	13.2976(6)	30.0579(15)	19.9085(15)
β (°)	94.646(2)	91.788(2)		99.724(2)
V (Å^3)	2639.5(3)	2754.2(2)	7312.8(8)	3333.0(4)
Z	2	4	3	4
ρ_{calc}, g.cm^{-3}	1.250	1.205	1.319	1.108
μ(Mo K$_\alpha$), mm^{-1}	0.233	0.091	0.099	0.065
F(000)	1056	1072	2880	1216
temp (K)	100(2)	100(2)	100(2)	100(2)
θ range (°)	2.379–27.499	3.009–28.282	2.887-27.087	2.926-26.818
data collected (h,k,l)	-12:11, -20:20, -22:22	-17:17, -20:20, -17:17	-21:21, -21:21, -38:38	-9:10;-24:25; -24:25
min, max transm	0.6364 , 0.7461	0.7224, 0.7465	0.7058,0.7457	0.6454, 0.7454
rflns collected	106038	134350	44691	35087
indpndt reflns	6073	6845	3461	7106
observed reflns $F_o \geq$ 2.0 σ (F_o)	4342	5804	2906	4686
R(F) (%)	4.94	4.10	3.60	5.37
wR(F^2) (%)	10.34	10.68	8.37	11.17
GooF	1.024	1.033	1.036	1.015
weighting a,b	0.0458, 2.4506	0.0569, 1.2485	0.0382, 9.4286	0.0431, 3.6733
params refined	317	335	202	375
min, max resid dens	-0.263, 0.590	-0.316, 0.389	-0.192, 0.354	-0.250, 0.391

Notes and references

[a]*Stratingh Institute for Chemistry, University of Groningen Nijenborgh 4, 9747 AG Groningen, The Netherlands, E-mail: edwin.otten@rug.nl.*

† Electronic Supplementary Information (ESI) available: NMR spectra for **1-K**, **2-K**, **2-Na**, **3-Na$_{THF}$**, **3-Na** and **1-Bu$_4$N**. See DOI: 10.1039/b000000x/

‡ Footnotes should appear here. These might include comments relevant to but not central to the matter under discussion, limited experimental and spectral data, and crystallographic data.

1. J. F. Hartwig, *Organotransition metal chemistry : from bonding to catalysis*, University Science Books, Sausalito, Calif., 2010.
2. A. d. Meijere, S. Bräse and M. Oestreich, eds., *Metal-Catalyzed Cross-Coupling Reactions and More*, Wiley-VCH, Weinheim, 2014.
3. P. J. Chirik and K. Wieghardt, *Science*, 2010, **327**, 794-795.
4. W. I. Dzik, J. I. van der Vlugt, J. N. H. Reek and B. de Bruin, *Angew. Chem. Int. Ed.*, 2011, **50**, 3356-3358.
5. V. Lyaskovskyy and B. de Bruin, *ACS Catal.*, 2012, **2**, 270-279.
6. V. K. K. Praneeth, M. R. Ringenberg and T. R. Ward, *Angew. Chem. Int. Ed.*, 2012, **51**, 10228-10234.
7. O. R. Luca and R. H. Crabtree, *Chem. Soc. Rev.*, 2013, **42**, 1440-1459.
8. M.-C. Chang, T. Dann, D. P. Day, M. Lutz, G. G. Wildgoose and E. Otten, *Angew. Chem. Int. Ed.*, 2014, **53**, 4118-4122.
9. M. C. Chang and E. Otten, *Chem. Commun.*, 2014, **50**, 7431-7433.
10. S. M. Barbon, P. A. Reinkeluers, J. T. Price, V. N. Staroverov and J. B. Gilroy, *Chem. – Eur. J.*, 2014, **20**, 11340-11344.

11. S. M. Barbon, J. T. Price, P. A. Reinkeluers and J. B. Gilroy, *Inorg. Chem.*, 2014.
12. L. Bourget-Merle, M. F. Lappert and J. R. Severn, *Chem. Rev.*, 2002, **102**, 3031-3066.
13. K. Gregory, P. Von Ragué Schleyer and R. Snaith, in *Adv. Inorg. Chem.*, ed. A. G. Sykes, Academic Press, 1991, pp. 47-142.
14. R. E. Mulvey, *Chem. Soc. Rev.*, 1998, **27**, 339-346.
15. A. Y. Robin and K. M. Fromm, *Coord. Chem. Rev.*, 2006, **250**, 2127-2157.
16. K. M. Fromm, *Coord. Chem. Rev.*, 2008, **252**, 856-885.
17. F. A. Neugebauer and H. Trischmann, *Justus Liebigs Ann.Chem.*, 1967, **706**, 107-111.
18. J. B. Gilroy, M. J. Ferguson, R. McDonald, B. O. Patrick and R. G. Hicks, *Chem. Commun.*, 2007, 126-128.
19. J. B. Gilroy, P. O. Otieno, M. J. Ferguson, R. McDonald and R. G. Hicks, *Inorg. Chem.*, 2008, **47**, 1279-1286.
20. J. C. Ma and D. A. Dougherty, *Chem. Rev.*, 1997, **97**, 1303-1324.
21. W. Clegg, E. K. Cope, A. J. Edwards and F. S. Mair, *Inorg. Chem.*, 1998, **37**, 2317-2319.
22. J. M. Smith, A. R. Sadique, T. R. Cundari, K. R. Rodgers, G. Lukat-Rodgers, R. J. Lachicotte, C. J. Flaschenriem, J. Vela and P. L. Holland, *J. Am. Chem. Soc.*, 2006, **128**, 756-769.
23. M. L. Cole, A. J. Davies, C. Jones and P. C. Junk, *J. Organomet. Chem.*, 2007, **692**, 2508-2518.
24. M. M. Rodriguez, E. Bill, W. W. Brennessel and P. L. Holland, *Science*, 2011, **334**, 780-783.
25. C.-L. Pan, W. Chen and J. Song, *Organometallics*, 2011, **30**, 2252-2260.
26. M. G. Davidson, D. Garcia-Vivo, A. R. Kennedy, R. E. Mulvey and S. D. Robertson, *Chem. – Eur. J.*, 2011, **17**, 3364-3369.
27. J. B. Gilroy, B. O. Patrick, R. McDonald and R. G. Hicks, *Inorg. Chem.*, 2008, **47**, 1287-1294.
28. S. Hong, L. M. R. Hill, A. K. Gupta, B. D. Naab, J. B. Gilroy, R. G. Hicks, C. J. Cramer and W. B. Tolman, *Inorg. Chem.*, 2009, **48**, 4514-4523.
29. R. Wizinger and V. Biro, *Helv. Chim. Acta*, 1949, **32**, 901-912.
30. H. Irving, J. B. Gill and W. R. Cross, *J. Chem. Soc.*, 1960, 2087-2095.
31. F. Beffa, P. Lienhard, E. Steiner and G. Schetty, *Helv. Chim. Acta*, 1963, **46**, 1369-1376.
32. S. Balt and W. E. Renkema, *J. Coord. Chem.*, 1977, **6**, 201-205.
33. A. R. Siedle and L. H. Pignolet, *Inorg. Chem.*, 1980, **19**, 2052-2056.
34. I. S. Gennadii, N. L. Galina and I. G. Pervova, *Russ. Chem. Rev.*, 2006, **75**, 885-900.
35. Bruker., *APEX2 (v2012.4-3), SAINT (Version 8.18C) and SADABS (Version 2012/1). Bruker AXS Inc., Madison, Wisconsin, USA.*, 2012.
36. G. Sheldrick, *Acta Crystallographica Section A*, 2008, **64**, 112-122.

Alkali-metal salts of formazanates are synthesized and their solid state and solution structures are determined. Dimeric, hexameric or polymeric aggregates are obtained, depending on the substitution pattern. The nitrogen-rich [NNCNN] backbone of formazanates leads to 4- and 5-membered chelate rings for these ionic compounds, which contrasts the 6-membered chelates found for more covalent complexes with these ligands.